Failure and Fracture Mechanisms of Injection-Molded Plastic Products

M. J. M. VAN DER ZWET, A. J. HEIDWEILLER

Department of Engineering Design, Faculty of Industrial Design Engineering, Delft University of Technology, Leeghwaterstraat 35, 2628 CB Delft, The Netherlands

Received 30 January 1997; accepted 9 August 1997

ABSTRACT: The effect of geometry transitions on the mechanical load-carrying ability of specimens has been studied. Special attention has been given to a potentially positive influence of the injection molding process. Tensile tests, three-point bending tests, and low cycle fatigue tests were performed on specimens with either drilled or molded-in holes. Tests were conducted at various temperatures and deformation rates. Two commercial grades of poly(methyl methacrylate) have been applied. To obtain a better understanding of the fracture mechanism, the fracture surface morphology was related to the molecular orientation investigated by the birefringence method and the results of a finite element method analysis. The extent of redistribution of stresses seemed considerable, even in the case of a brittle material like poly(methyl methacrylate). As a result, the linear theory is a safe, but very conservative, approach for the load-carrying ability of plastic products. It also seemed that injection molding may have a favorable influence on load-carrying ability. This result could be related to the fracture mechanism. © 1998 John Wiley & Sons, Inc. J Appl Polym Sci **67:** 1473–1487, 1998

Key words: stress concentration; geometry transition; injection molding; molecular orientation; fractography; geometry change

INTRODUCTION

Today, injection-molding technology allows mass production of plastic products at a low cost. Frequently, various functions are integrated into the product, resulting in a complex geometry with many geometry transitions. Based on experience, we know that geometry transitions very often are weak parts of products due to a local appearance of peak stresses combined with a triaxial stress state. It is also known that the injection-molding process may have a significant influence on the load-carrying ability of plastic products. Therefore, much research has been conducted on the (negative) effects of weld lines.[1,2] The positive effects of the skin layer, with a morphology that is strongly influenced by the high cooling rate at the mold walls, have also been studied.[3–8] Much of this research is related to semicrystalline polymers.[3–7] In general, for semicrystalline polymers, the nature of the crystalline regions are influenced by the injection-molding process. Furthermore, residual stresses caused by nonuniform temperature distribution during packing and subsequent cooling may influence the load-carrying ability.

Although a better understanding of the load-carrying ability of (injection-molded) geometry transitions in plastic products would offer considerable financial profit, little research on this subject has been performed. Undoubtedly, this is due to the fact that, in itself, the load-carrying ability of simple plastic specimens is difficult to predict because of time and temperature dependency of polymeric materials. Besides, the costly mold necessary for manufacturing specimens with injection-molded geometry transitions impedes the re-

Correspondence to: A. J. Heidweiller.

Journal of Applied Polymer Science, Vol. 67, 1473–1487 (1998)
 CCC 0021-8995/98/081473-15

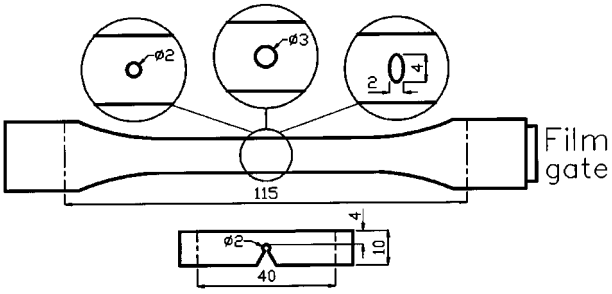

Figure 1 Tensile and three-point bending specimens.

search on the combined effect of injection molding and geometry transitions.

Research on the load-carrying ability of geometry transitions often has been conducted on machined blunt notches.[9–13] Frequently, the results are presented in terms of a notch factor or notch sensitivity, but in fact there is no good model to predict the load-carrying ability of such simple geometry transitions.

The effect on load-carrying ability of injection-molding conditions has been studied mainly on smooth specimens, machined from injection-molded plates. Orientation is affected by injection-molding conditions and, contrary to plates from drawn material, the orientation is not homogeneously distributed over the cross section.[14] Hoare and Hull[15] report that craze initiation and crack initiation afterward in specimens cut from injection-molded polystyrene plates occurred in the area of minimum orientation for angles between tensile load and flow direction smaller than 70°. Minimum orientation was in the middle of the plates. Furthermore, the craze initiation stress seemed to be at the same level for unoriented material (40 MPa), which corresponds to the low level of orientation found in the middle of the plate. They observed that crazes do not grow into highly oriented areas (stable crazes), which has also been reported by other researchers.[1,16]

Rather extensive research has been conducted on specimens with sharp notches or cracks, starting from a fracture mechanics approach and also taking into account orientation effects.[17] Such research first of all serves materials science and is only indirectly important for product designers.

The combined effect of injection molding and geometry transitions has been studied by various authors using specimens with simple molded-in geometry transitions.[2,5,6,8,18] Much attention has been given to weld lines,[2] but the positive effect of the skin layer also has been studied.[5,6,8] Crawford et al.[6] compared the fatigue load-carrying ability of acetal copolymer specimens having molded-in notches or holes with specimens of the same geometry having machined geometry transitions. They reported that the former specimens withstand a higher number of cycles. This is explained by the fact that the peak stress of the geometry transition is just located at the tough skin layer. Corresponding results are reported for Izod impact strength on poly(butylene terephthalate) specimens.[5] Hobbs and Pratt[5] also observed a positive effect of increasing skin thickness on impact strength.

The current research concentrates on products with circular or elliptical holes. Weakening due to holes is a common factor in product design. Furthermore, circular holes do have a rather high stress concentration and can be machined quite easily. The influence of different types of holes on the load-carrying ability has been investigated. Furthermore, the difference between molded-in holes and machined holes has been analyzed. A special mold with different mold inserts had to be built, which made it possible to produce specimens with a range of molded-in holes.

EXPERIMENTAL

Materials

Both applied grades of poly(methyl methacrylate) (PMMA) are appropriate for injection molding. They will be indicated with grade H and grade L. Grade H has a weight average molar mass, $\overline{M_w}$

Table I Injection-Molding Conditions

Processing Condition	Grade H	Grade L
Nozzle temperature	250°C	260°C
Hydraulic pressure during filling	60 bar	60 bar
Hydraulic pressure during packing	60 bar	20 bar
Pack time	18 s	12 s
Cool time	20 s	41 s

Table II Overview of All Experiments

Material Grade	Type of Test	No. of Specimens	Speed, Frequency	Temperature (°C)	Geometry Hole (mm)	Manufacturing of Hole	Treatment
H	Tensile	240	5, 50, 500 mm min^{-1}	23, 40	2, 3, ellipse	Molded-in	Annealed
H, L	Tensile	110	5 mm min^{-1}	29, 23	2, 3	Drilled, molded-in	Annealed, as-molded
L	3-point bending	40	5–4300 mm min^{-1}	23	2	Drilled, molded-in	Annealed
L	Low cycle fatigue	175	0.2 Hz	23	3, ellipse	Drilled, molded-in	Annealed

$= 1.7\ 10^5$ g mol^{-1}. Grade L has a rather low molar mass, with $\overline{M_w} = 0.84\ 10^5$ g mol^{-1} and $\overline{M_n} = 0.36\ 10^5$ g mol^{-1}. According to Vincent[19] and Kusy and Turner,[20] the fracture strength and fracture energy will not reach the constant level. This explains why the material behavior of grade L is more brittle than grade H.

Specimens

The specimen geometry is based on ISO/R 527 type 1, as indicated in Figure 1 (cross section is 4×10 mm^2, and initial clamping distance is 115 mm). Five different types of specimens were applied:

1. Plain injection-molded specimens.
2. Injection-molded specimens containing a central drilled hole of 2 or 3 mm diameter.
3. Injection-molded specimens containing a central molded-in circular hole of 2 or 3 mm diameter.
4. Injection-molded specimens containing a central molded-in elliptical hole of 2×4 mm.
5. Three-point bending specimens.

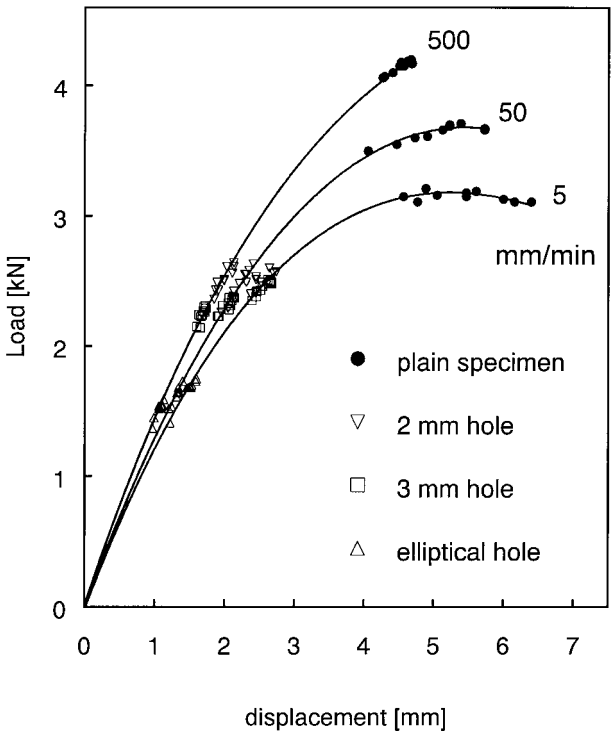

Figure 2 Typical load-displacement curves of PMMA grade H at 23°C. Markers indicate fracture points of all individual test specimens.

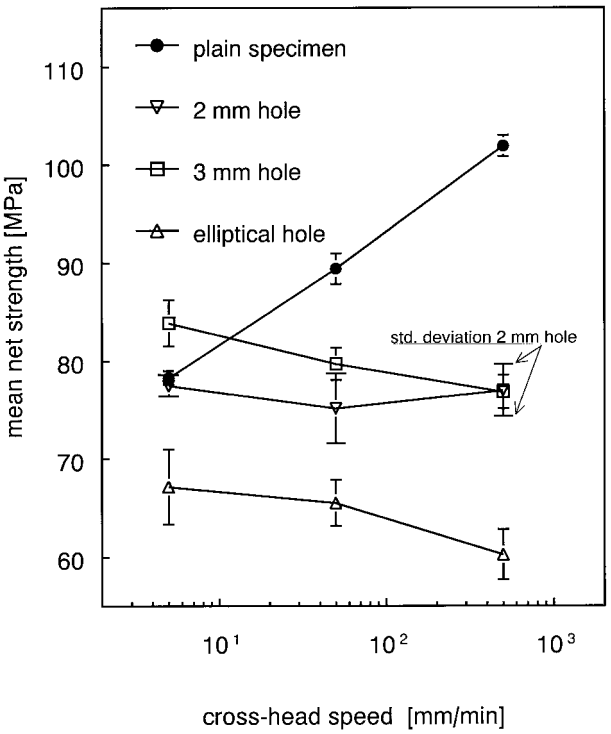

Figure 3 Mean net strength as a function of cross-head speed.

Specimens for the three-point bending tests were made from tensile specimens containing a (drilled or molded-in) hole of 2 mm (as indicated in Fig. 1). Both ends were removed, leaving a straight specimen of 60 mm in length. A saw cut was made from one side to the hole, creating a blunt notch of 6 mm in depth and 1 mm radius. The remaining width is 4 × 4 mm. The small draft angle of the sides was milled away to obtain a rectangular cross section. The applied span was 40 mm.

A mold and different mold inserts were used for injection molding the specimens. The mold has a film gate (Fig. 1). Grade H specimens were injection-molded with an Arburg 150, and grade L specimens were injection-molded with an Arburg 270. The processing conditions are indicated in Table I.

To avoid warming up and melting during drilling, the holes were drilled under water. Most of the specimens were annealed before testing to reduce the residual stresses that originate from injection molding. The specimens were annealed for 16 h at 90°C, preceded by slow warming up and followed by slow cooling (10°C/h). The annealing temperature is below the glass rubber transition temperature; therefore, the molecular orientation was not altered by the annealing process.

Fracture Experiments

Experiments were conducted at different temperatures and deformation rates using both annealed and as-molded specimens. A summary of all experiments is given in Table II. Tensile tests were conducted at 23, 29, and 40°C and at cross-head speeds of 5, 50, and 500 mm min^{-1}. Three-point bending tests were performed at 23°C and at cross-head speeds of 5, 50, 470, and 4300 mm min^{-1}. Fatigue tests were conducted at 23°C and at a very low frequency of 0.2 Hz to avoid unacceptable heating of the specimens during the test. A sinusoidal tensile loading was used with its minimum at 0 MPa (load ratio $R = 0$).

Most tensile tests were performed on a MTS 80 hydraulic machine. The tests at 23°C in the second row of Table II were conducted on a hydraulic machine that was built according to our own specifications. The latter has also been used for the fatigue tests. Three-point bending tests were performed on a specially designed hydraulic three-point bending set-up.

Table III Theoretical Stress Concentration Factors K_t and Average Value of Notch Factors K_s over 10 Data Points for 23°C and 40°C

		K_s at 23°C			K_s at 40°C		
	K_t	5 mm min^{-1}	50 mm min^{-1}	500 mm min^{-1}	5 mm min^{-1}	50 mm min^{-1}	500 mm min^{-1}
Ellipse	3.50	1.17 (2%)	1.36 (4%)	1.69 (4%)	0.92 (5%)	1.13 (5%)	1.37 (4%)
2 mm	2.51	1.01 (3%)	1.19 (5%)	1.32 (4%)	0.86 (2%)	1.03 (4%)	1.10 (3%)
3 mm	2.35	0.93 (5%)	1.12 (3%)	1.33 (4%)	0.82 (5%)	0.91 (2%)	1.07 (5%)

Coefficient of variation appears in parentheses.

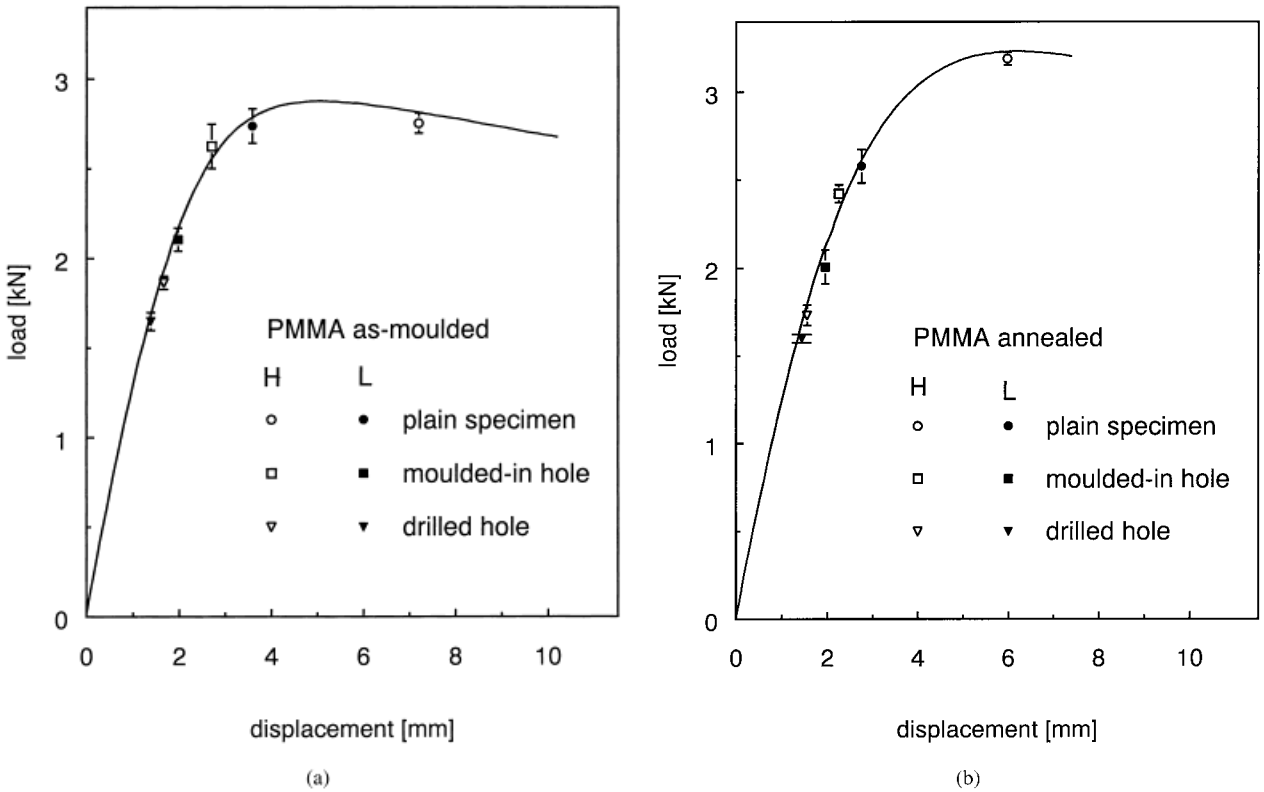

Figure 4 Typical load-displacement curves of plain grade H specimens tested at 23°C and 5 mm min^{-1}: (a) as-molded; (b) annealed. Markers indicate the average fracture load and average strain at fracture for different specimen types.

Fracture Surfaces and Birefringence Measurements

All fracture surfaces have been studied using an optical microscope (Jenavert) with magnifications up to 500×. In addition, a scanning electron microscope (Jeol 840 A) was used.

To investigate the molecular orientation, the optical birefringence has been measured using a specially equipped optical microscope with linear polarized light (Jenapol) and an Ehringhaus E6 tilting compensator.

RESULTS AND DISCUSSION

Tensile Tests

Tensile Specimens with Molded-In Holes

The aim was to find out how much the load-carrying ability of tensile specimens is affected by molded-in holes with various contours. The tests concerned are summarized in the first row of Table II. The applied material is PMMA grade H. The tests have been conducted at cross-head speeds of 5, 50, and 500 mm min^{-1} and temperatures of 23° and 40°C. Ten tests have been performed for each test condition.

In Figure 2, three typical load-displacement curves of smooth specimens are shown for cross-head speeds of 5, 50, and 500 mm min^{-1} and a temperature of 23°C. The fracture points of the specimens with a hole are also indicated. It is pointed out that displacement of the specimens is hardly influenced by the relative high strains near the hole.

First of all, the decrease of load-carrying ability of specimens with a hole can be partly explained by the decrease of net section. There is also the effect of stress concentration as illustrated in Figure 3, where the mean net strength (average value over 10 data points) and the standard deviation are plotted as a function of cross-head speed. From the linear relation of the smooth specimens, it can be concluded that the fracture process essentially is a rate process. Specimens with a hole do not show such a positive linear correlation. The mean net strength even tends to decrease with increasing cross-head speed. This can be explained by a decrease of (nonlinear) deformation capacity at increasing cross-head speeds, re-

Table IV Notch Factors of Specimens with a Drilled Hole and Specimens with a Molded-In Hole at Different Test Conditions

Temperature	Grade	Type of Specimen	K_s Drilled	K_s Molded-In	Ratio K_s[a]
23°C	L	2 mm hole; as molded	1.33 (5%)	1.04 (5%)	1.28
		2 mm hole; annealed	1.29 (4%)	1.03 (6%)	1.26
23°C	H	2 mm hole; as molded	1.22 (3%)	0.87 (5%)	1.41
		2 mm hole; annealed	1.48 (4%)	1.06 (2%)	1.40
29°C	H	2 mm hole; as molded	0.99 (3%)	0.83 (2%)	1.20
		2 mm hole; annealed	1.29 (4%)	1.03 (1%)	1.26
		3 mm hole; as molded	0.92 (2%)	0.81 (2%)	1.13
		3 mm hole; annealed	1.20 (1%)	0.92 (5%)	1.30

Coefficient of variation appears in parentheses.
[a] Ratio K_s = K_s drilled hole/K_s molded-in hole. This ratio is the same as the ratio of the nominal strength of both specimens.

sulting in a lower amount of redistribution of stresses near the hole.

To indicate the effect of stress concentrations, often the notch factor K_s is applied:

$$K_s = \sigma_{TS}/\sigma_r \quad (1)$$

where σ_{TS} is ultimate tensile strength and σ_r is mean net-section strength.

Frequently, the notch factor is compared with the theoretical stress concentration factor K_t. This factor indicates the maximum stress according to linear elastic theory:

$$K_t = \sigma_{\text{max,lin.elast.}}/\sigma_N \quad (2)$$

where $\sigma_{\text{max,lin.elast.}}$ is maximum principal stress and σ_N is nominal (mean net-section) stress.

In Table III, the mean values of the notch factors are indicated. As was expected, an increase of K_t results in an increase of K_s. The ellipse does have the highest notch factor. Further, it is pointed out that the strength reduction of this brittle material cannot be neglected, however, it is rather low at the applied conditions. At low cross-head speeds and/or high temperatures, the notch factor even decreases to values <1, which is denoted as "notch strengthening" (mean net strength higher than ultimate tensile strength). Starting from a linearization of formula (1), the following approximation can be established for the coefficient of variation of the notch factor:

$$V^2(K_s) \approx V^2(\sigma_{TS}) + V^2(\sigma_r) \quad (3)$$

where $V(K_s)$ denotes coefficient of variation of K_s, etc.

As can be seen in Table III, the coefficient of variation of the K_s values is rather low. The maximum is 5%.

Distinction Between Specimens with Molded-In Holes or Drilled Holes

To investigate how much the notch factor is influenced by the molding-in of the holes, a new series of tensile tests was conducted, applying specimens with molded-in holes and drilled holes (second row of Table II). The cross-head speed was 5 mm min^{-1}, and five tests were conducted per test condition. Both annealed and as-molded specimens were applied. The tests at 23°C were performed with both PMMA grades, but only a 2 mm hole diameter was applied as geometry transition. The tests at 29°C were conducted with specimens having hole diameters of 2 or 3 mm and manufactured from PMMA grade H.

In Figure 4, typical load-displacement curves of smooth PMMA grade H specimens tested at 23°C are presented, both for as-molded and annealed specimens. Also, for each test condition and both PMMA grades, the combination of average fracture loading and average fracture displacement (over five data points) is plotted. The tensile curve of PMMA grade L follows the curve of grade H rather precisely, but as can be seen in Figure 4, the specimens fracture at a lower loading. It can be noted from Figure 4 that, in general:

- Specimens with molded-in holes have a higher load-carrying ability than specimens with drilled holes.
- The difference in load-carrying ability is higher for the grade H specimens than for the grade L specimens. Presumably, the higher molar mass of grade H enables more orientation during the injection-molding process. In-

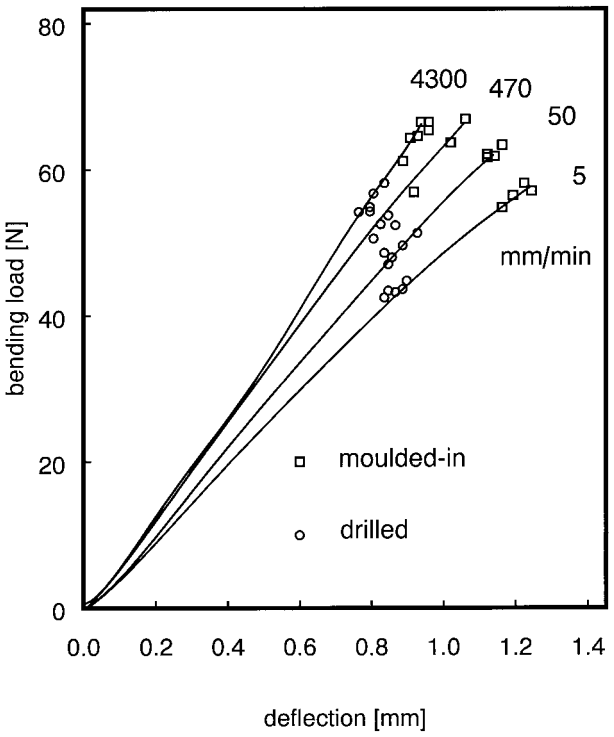

Figure 5 Typical three-point bending curves of grade L. Markers indicate fracture load-deflection points for three-point bending specimens with drilled and molded-in blunt notch.

deed, grade H specimens show a higher level of birefringence near the hole than the grade L specimens (both for annealed and for as-molded specimens).

- The load-carrying ability of grade H specimens is higher than of grade L specimens. This also applies to specimens with a geometry transition.
- Annealing of grade L specimens slightly lowers the load-carrying ability.
- Annealing of grade H smooth specimens results in a higher strength. However, for the specimens with a geometry transition, annealing results in a lower load-carrying ability, which of course is a consequence of the lower amount of redistribution of stresses. The latter also applies to the specimens tested at 29°C.

Results of the tests are summarized in Table IV. The K_s values are average values over five data points, and all of the tests are conducted at 5 mm min^{-1}. The scatter of the notch factor is rather low, as found in Table III. The following can be concluded from Table IV:

- The notch factor of the drilled holes is considerably higher than the notch factor of the molded-in holes. The drilled holes, in particular, may cause a substantial decrease of load-carrying ability.
- K_s values again are much lower than K_t values. This also applies to the drilled holes.
- Annealing results in a higher notch factor for grade H. This is mainly caused by an increase in ultimate tensile strength, as can be concluded from Figure 4. A similar conclusion can be drawn from our results for an increase in cross-head speed (see Fig. 2) or a decrease in temperature.

The notch factors for PMMA, as reported in literature,[9,10] do not differ very much from the notch factors previously described. Takano and Nielsen[9] found a notch factor of 1.64 (K_t is 2.05) for PMMA specimens with double-sided notches (probably machined), tested under similar conditions as the current tests. Prabhakaran and colleagues[10] found a notch factor of 1.49 (K_t is 2.68) for double-sided, semicircular machined notches. Fraser and Ward[12] suggested a linear relation between K_s and K_t for machined blunt notches, but

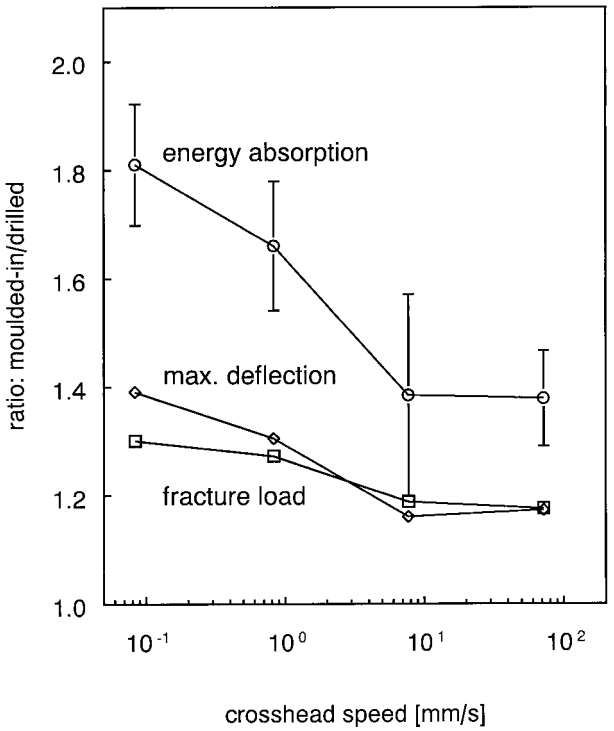

Figure 6 Relation between the results of three-point bending specimens with a notch made by drilling and a notch made by molding-in. The average values for each series are applied.

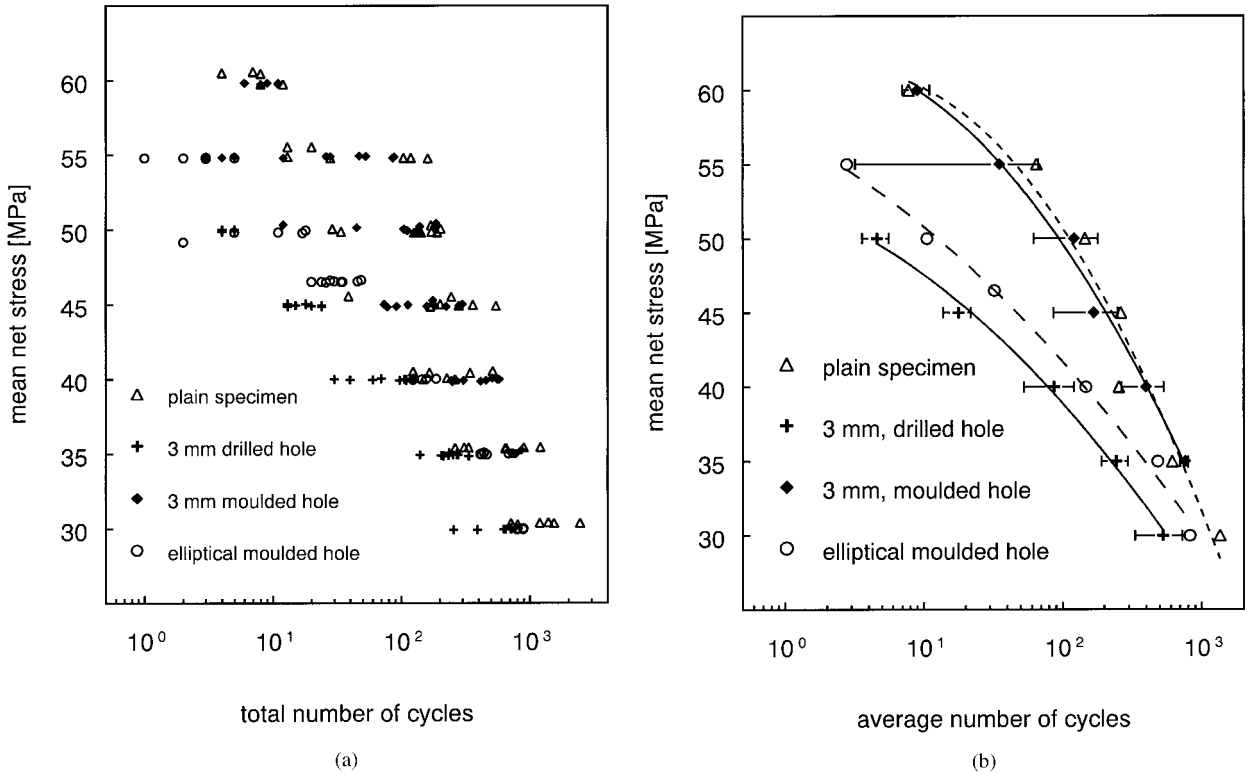

Figure 7 Low cycle fatigue S–N data of annealed grade L specimens: (a) data points; (b) mean values and curve fits.

this does not correspond with the results of the references previously described.[9,10] We conclude herein that an analysis based on notch factors may give more insight into the load-carrying ability behavior, but it is too simple a starting point for a quantitative model of the loading behavior of geometry transitions. The notch factor depends on the test condition and is not in a simple way related to the theoretical stress concentration factor, perhaps with the exception of very brittle material behavior. Better possibilities for arriving at a quantitative model for geometry transitions are offered by models that take into account the nonlinear constitutive behavior combined with a critical value for either the hydrostatic component of the stress tensor or the maximum principal stress.[21,22]

Three-Point Bending Tests

The specimens were machined from PMMA grade L tensile specimens with molded-in or drilled holes of 2 mm (Fig. 1 and Table II), followed by annealing. Rather low cross-head speeds of 5, 50, 470, and 4300 mm min^{-1}, respectively were used. Based on linear-elastic theory and taking into account the effect of stress concentrations, this is equivalent to a 14 times higher local strain rate than in the applied tensile specimens tested with identical cross-head speeds. Four to five tests were conducted for each test condition. No tests have been performed on smooth specimens.

Typical load-deflection curves are presented in Figure 5. The fracture points of the individual specimens are also plotted in the figure. The specimens with drilled holes again have a substantially lower load-carrying ability than the specimens with injection-molded holes. However, the difference in load-carrying ability is higher for low cross-head speeds. The deflection at fracture of the specimens with drilled holes is hardly influenced by the cross-head speed (nominal fracture strain ~11%), whereas for the specimens with molded-in holes the deflection at fracture decreases considerably with increasing cross-head speed.

Based on previously described data, the energy absorption (i.e., the area under the bending load-deflection curve) must differ considerably in the case of low cross-head speeds. This is illustrated in Figure 6, where for the energy absorption, the ratio between specimens with molded-

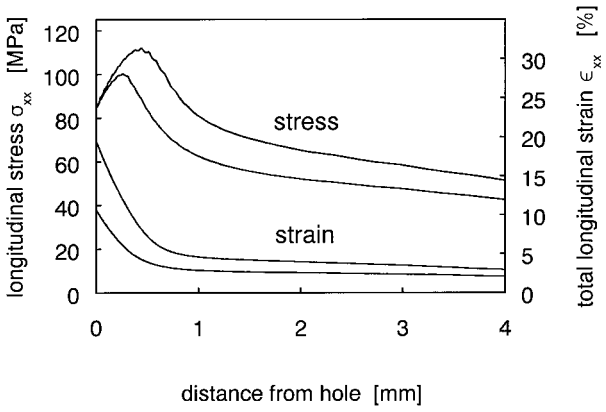

Figure 8 Stress distribution in a grade H-annealed tensile specimen, at one side of a 2 mm hole, according to FEM. Temperature is 29°C, and cross-head speed is 5 mm min^{-1}.

in holes and drilled holes is plotted as a function of cross-head speed. In Figure 6, the average value of the data points per test condition is applied. Also, in Figure 6, the ratios for the parameter "fracture load" and "maximum deflection" are plotted. In case of fracture load, the ratio also can be interpreted as a ratio of notch factor. At high strain rates, the ratios seemed to decrease to a constant level. This is not investigated further because of the increasing bouncing effect at higher strain rates. It is pointed out that, according to Figure 6, even at high strain rates the energy absorption—which is a very important design parameter—of the specimens with molded-in holes is 40% higher than the specimens with drilled holes. Based on the tensile test results, greater differences are expected for PMMA grade H.

Low Cycle Fatigue Tests

Low cycle fatigue tests were conducted at 23°C using annealed PMMA (grade L) specimens (Fig. 1). A sinusoidal tensile loading (load ratio $R = 0$) with a frequency of 0.2 Hz was applied. At this frequency, no heating of the specimen could be detected, as was measured with an Ultrakust infrared sensor. The specimens used in the tests were: plain specimens, specimens with a drilled hole of 3 mm, specimens with a molded-in hole of 3 mm, and specimens with a molded-in elliptical hole. Because of the time-consuming nature of the fatigue tests, a selection was made concerning the number of tested specimens for every set of data points.

The test results show wide scatter as can be seen in Figure 7(a). This especially applies to the plain specimens and at higher amplitudes to the specimens with a molded-in hole. Standard deviations for the specimens with a hole of 3 mm are indicated in Figure 7(b). Because of the wide scatter in lifetime, we restrict ourselves to a discussion of the tendencies of the results. Therefore, the average values for every type of specimen are plotted in Figure 7(b). A second-order polynomial has been used to fit the data. Continuous lines are used for the specimens with a 3 mm hole. Discontinuous lines are used for the smooth specimens and for the specimens with an elliptical hole. It can be seen that the average number of cycles is nearly equal for plain specimens and specimens with a molded-in hole of 3 mm ($K_s \sim 1$). The specimens with a drilled hole always have the lowest average strength, even lower than the specimens with an elliptical hole, having a 1.5 time higher theoretical stress concentration factor.

The curves converge at lower amplitudes, taking into account the logarithmic horizontal scale. However, at an amplitude of 35 MPa, the average number of cycles to fracture of the specimens with drilled hole is still three times lower than of the specimens with a molded-in hole of 3 mm. A similar tendency can be observed in Crawford and colleagues[6] for tensile fatigue tests on an acetal copolymer in the range of 10^4–10^7 cycles to fracture. The S-N curve for specimens with a drilled hole approaches the curve of the plain specimens for an increasing number of cycles, whereas the curve of the molded-in hole specimens even crosses the plain specimen curve (notch strengthening). Specimens with a transverse molded-in V-notch show notch strengthening in the entire test range.

Fracture Surface Morphology

General

PMMA is a rather brittle polymer. Fracture takes place due to breakdown of one or more crazes and, generally, the fracture surface is perpendicular to the direction of the highest principal stress.[23] At the fracture surface, the remainder of the craze can be observed as a highly reflecting zone (mirror zone), with a more or less concentric shape. In the center of the mirror zone, the location of fracture initiation can be identified easily using an optical microscope and, of course, this location is an important feature of the fracture mechanism. Because of the transparency of PMMA, combined with a difference in the refractive index of bulk

and craze material, optical microscopy can be used very well to analyze the morphology of the fracture surface.

A finite element method (FEM) analysis was conducted for annealed grade H specimens with a hole of 2 mm and loaded with 5 mm min^{-1} at 29°C. The evaluation was performed with the code MARC, applying a 20-node element. The deformation behavior was modeled as elastic-plastic with isotropic hardening, because there is no appropriate three-dimensional viscoelastic model available. Important input parameters were: yield point of 29.63 MPa at 1% (uniaxial) strain; ideally plastic Von Mises stress of 72.77 at 5% (uniaxial) strain; and a Poisson ratio of 0.38. Figure 8 shows the resulting distribution of stress σ_{xx} and strain ε_{xx} in the axial direction in the midplane of the specimen for two loads: σ_N = 56.39 MPa (average strength of drilled holes) and σ_N = 68.66 MPa (average strength of molded-in holes). The highest strains are at the hole surface. This also applies to the stresses in the elastic region; but, as can be seen in Figure 8, at higher loads, the peak stress will move from the hole surface, due to the increasing nonlinear behavior of the material.

Tensile Specimens with a Drilled Hole

As shown in Figure 9, two different types of mirror zones have been found at fracture surfaces of tensile specimens with a drilled hole. In our opinion, the type of mirror zone shown in Figure 9(a) is typical for geometry transitions.[24] The contour of the mirror zone is elliptical, so to some extent it follows the stress distribution. Around the initiation point is a circular area with radial boundaries between patches, whereas outside this area the structure is more elliptical. The diameter of the circular area seems to be rather independent of the test conditions (300–400 μm for grade H and ~160 μm for grade L). The initiation point of this type of fracture was often at some distance from the hole surface.

Narishawa and colleagues[21] assumed that the mean normal stress controls fracture, and starting from ideally plastic behavior and a plane strain situation, the location of the crack initiation point was used to calculate a critical mean normal stress. In Heidweiller,[22] a clear relation is shown between the location of the fracture initiation point and the location of the highest principal stress at fracture, as was calculated by FEM. The distance from the hole surface increases with increasing hole diameter and more ductile conditions (higher test temperature, no annealing, and lower loading rate). From FEM analysis, it seemed that the location of the highest mean normal stress is quite close to the location of the highest principal stress.

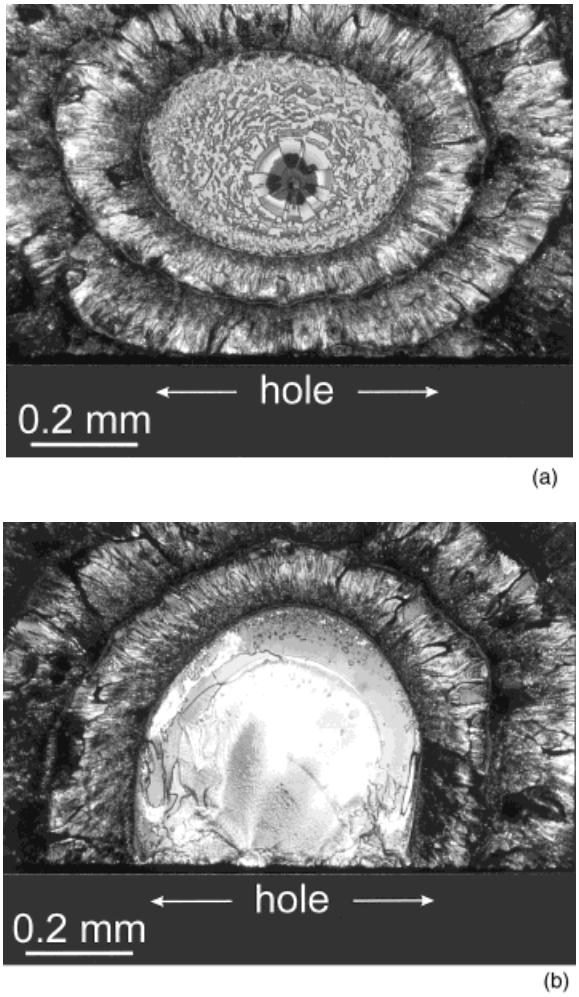

Figure 9 Typical mirror zones of fracture surfaces of tensile specimens having a drilled hole.

The fracture surface of Figure 9(b) exhibits a half concentric structure, and the fracture initiation is always at the hole surface. It leads to the assumption that this type of fracture is caused by flaws at the hole surface due to machining. For specimens with evident surface defects, this fracture type was confirmed. It is noteworthy that characteristics of the fracture surface of Figure 9(b) correspond with those of the plain specimens.

The fracture surface of Figure 9(a) has been found for both grades of PMMA; but, for the conditions described in our article, it was found only for PMMA grade H. This can be explained by the more brittle behavior of PMMA grade L concluded

from the tensile curves of Figure 4. Therefore, the material is more sensitive to surface defects.

Tensile Specimens with a Molded-In Hole

Four different regions of crack initiation could be distinguished for specimens with a molded-in hole (both circular and elliptical), as indicated in Figure 10(a). These regions are:

- Region 1: at the edge of hole surface and specimen side [Fig. 10(b)].
- Region 2: close to this edge, at small distance from the hole and side [Fig. 10(c)].
- Region 3: Near the center of the fracture surface [Fig. 10(d)].
- Region 4: At a side of the specimen. At very ductile conditions, geometrical discontinuities arise at the sides of the specimen from substantial plastic deformation. Fracture then initiates at such a discontinuity. In these cases, substantial notch strengthening was found ($K_s < 1$).

In fact, there is a fracture surface at both sides of the hole; but, in Figure 10(b–d), only that part is shown where the crack initiates.

The location of fracture initiation highly depends on the test conditions. With increasing ductility (higher test temperature, no annealing, and lower loading rate), the fracture location is shifted from location 1 through 2 and 3 to finally 4. Moreover, from tests conducted at 40°C, with specimens having a molded-in hole of 2 mm, it seemed—for the initiation points of region 2—that the distance of initiation points from the hole surface increases with decreasing cross-head speeds, resulting in more ductile behavior.

Fracture Mechanisms of Tensile Specimens with Drilled and Molded-In Holes

Because of the brittle nature of the fracture process and the inhomogeneous stress distribution near the hole, the local situation at the peak stress area is very important. Advantageous molecular orientation in the peak stress region forces fracture to initiate in a region of lower stresses. Therefore, the location of fracture initiation is an important feature of the failure process.

In Figure 11, a summary is given of the locations of initiation points in PMMA grade H specimens tested at 29°C at a cross-head rate of 5 mm min^{-1}. The regions as described in Figure 10(a) can be clearly distinguished. With respect to the annealed specimens with a 2 mm hole, it is noted that the crack initiation point of four out of five specimens was in region 2. The median of the distance from the hole was 0.3 mm, which is a bit lower than the peak stress distance of 4.4 mm (shown in Fig. 8). The open markers representing specimens with drilled holes show that:

- Fracture initiates in the middle of the specimens, where the molecular orientation has a minimum. This corresponds with Hoare and Hull.[15] However, it may also be important that the constraint arrives at a maximum in the middle.
- If fracture initiates at a certain distance from the hole, the distance is greater for specimens with a hole of 3 mm than for specimens with a hole of 2 mm. From FEM analysis, it is known that the same applies to the peak stress.

Obviously, the shape and position of the mirror zone for specimens with a molded-in hole are strongly influenced by the molecular orientation originating from injection molding.

Molecular Orientation. To get an indication of the orientation near the molded-in hole, birefringence measurements were conducted on a 1-mm-thick sample taken from the middle of a PMMA grade H specimen with a 2 mm hole (Fig. 12). Another sample was taken at the same position from a plain specimen. Birefringence is not only caused by molecular orientation, but also by (frozen-in) residual stresses. The interpretation of the results is complicated by the fact that, in PMMA, the contribution of the residual stresses is relatively high.[23] However, the birefringence measurements were conducted on specimens annealed below T_g. In addition, a good qualitative correspondence was found with birefringence measurements on polystyrene specimens (which will be published later), having a much lower optical coefficient for residual stresses, relative to the coefficient for orientation, than PMMA.[25] Therefore, it is assumed that residual stresses have little effect on the birefringence measurements.

The results plotted in Figure 12 are characteristic for injection-molded parts. Starting from the surface, the maxima in orientation originate from straining in the fountain flow, shear flow along a solidified layer at the cavity wall, and shear flow during packing.[14] Orientation in the plain speci-

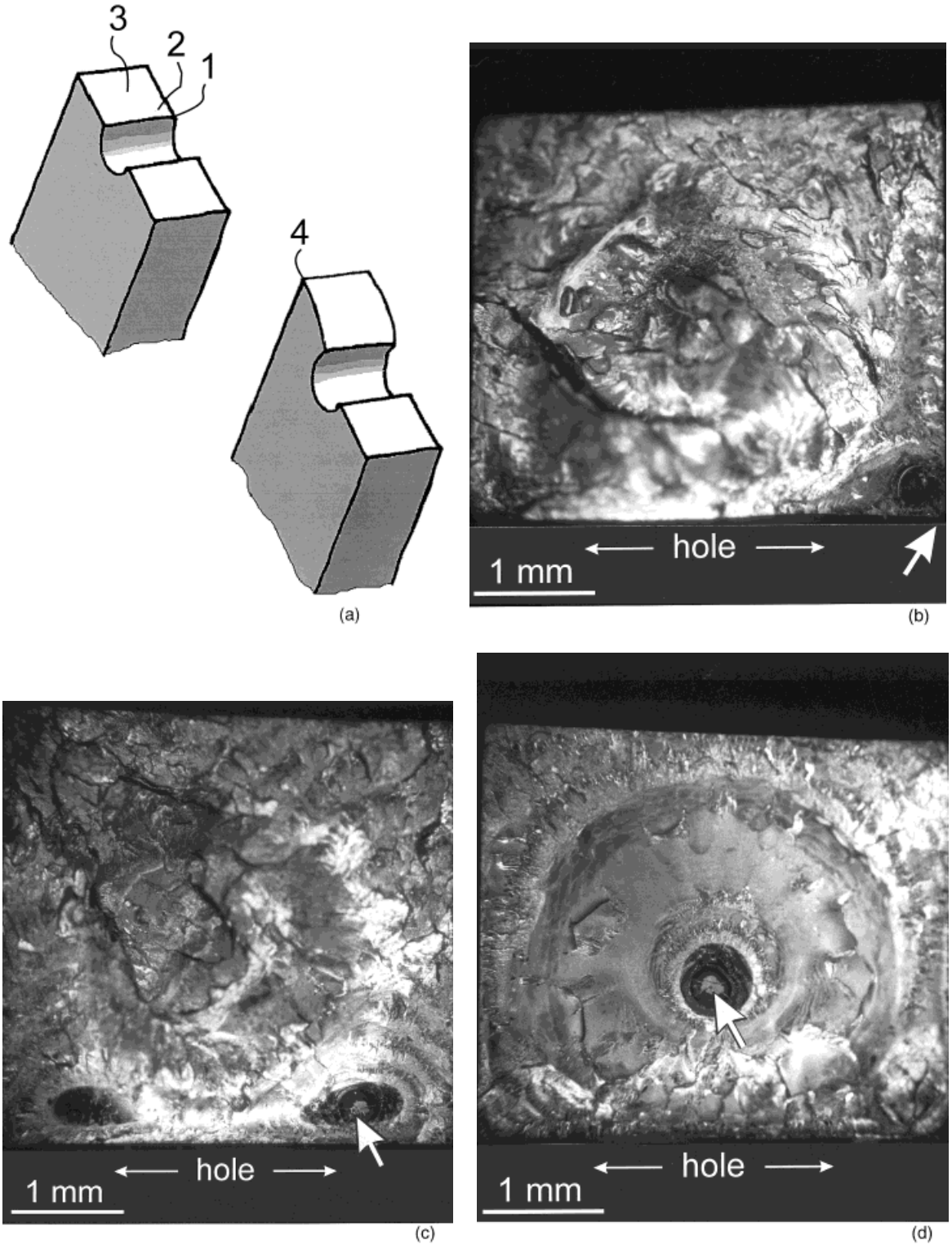

Figure 10 Fracture surfaces of PMMA grade H specimens with a molded-in hole. All samples are gold-coated. (a) Four regions of crack initiation, (b) region 1 (3-mm hole), (c) region 2 (2-mm hole), and (d) region 3 (3-mm hole).

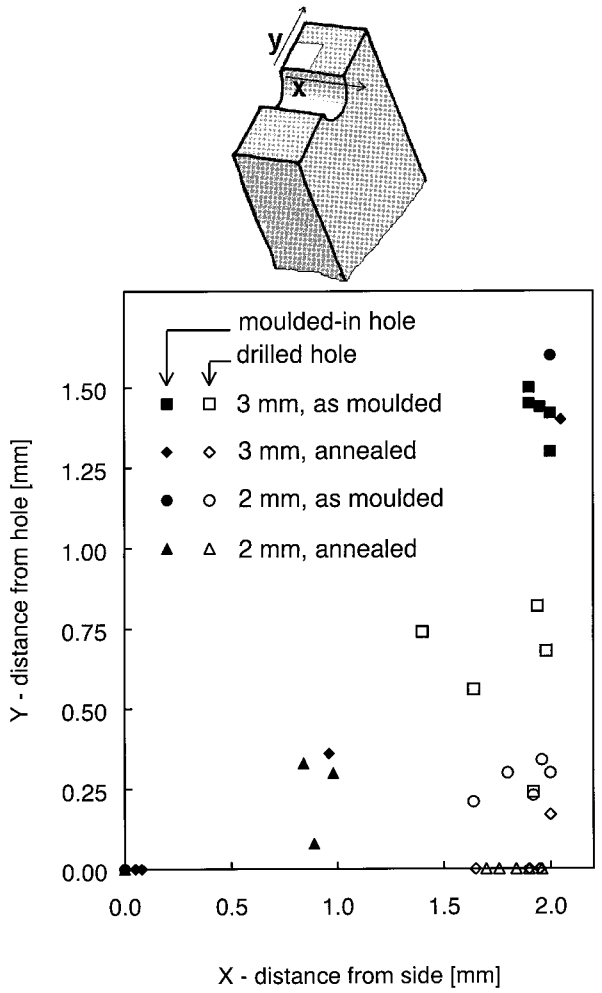

Figure 11 Plot of the initiation points of the tensile tests of PMMA grade H at 29°C and 5 mm min^{-1}.

men is only high near the surface. This means that little or no orientation will be present near the drilled holes, except at the hole ends. On the contrary, the molded-in hole exhibits a substantial amount of orientation near the hole surface. Orientation reaches a minimum in the middle between the hole and the side of the specimen.

Geometry Transition and Molecular Orientation. From previously described data, we conclude that the fracture mechanism of Figure 10(d) is highly determined by orientation distribution. This fracture surface, found in PMMA grade H specimens mostly as-molded, has a fracture initiation point in the area of minimum orientation, at least 1.3 mm from the hole surface. This corresponds with the observations on smooth specimens.[15,16] In specimens with a drilled hole tested under similar conditions, fracture initiates closer to the hole surface (Fig. 11).

Under conditions where the material exhibits more brittle behavior, the location of fracture initiation is in region 2 [Fig. 10(c)] rather than in region 3 [Fig. 10(d)]. Obviously, this is due to the stress field having a more peaked maximum closer to the hole surface. The fracture initiation points of specimens with a drilled hole tested under similar conditions are mostly at the hole surface. Because the region of fracture initiation points of Figure 10(c) (region 2) is not half the thickness of the specimens, but more at the ends of the hole, we conclude that there is a minimum in molecular orientation in that region. This also applies to the edges where the mechanism of Figure 10(b) (region 1) has its fracture initiation point.

Fracture Surfaces of Other Specimens

Three-Point Bending. Specimens with a drilled hole always showed fracture initiation half-way along the hole at the hole surface. In case of the lowest applied cross-head speed of 5 mm min^{-1}, the specimens with a molded-in hole showed fracture initiation at some distance from the hole, showing resemblance to Figure 10(c). At higher loading rates, fracture initiates at the hole surface that corresponds to the relatively high strain

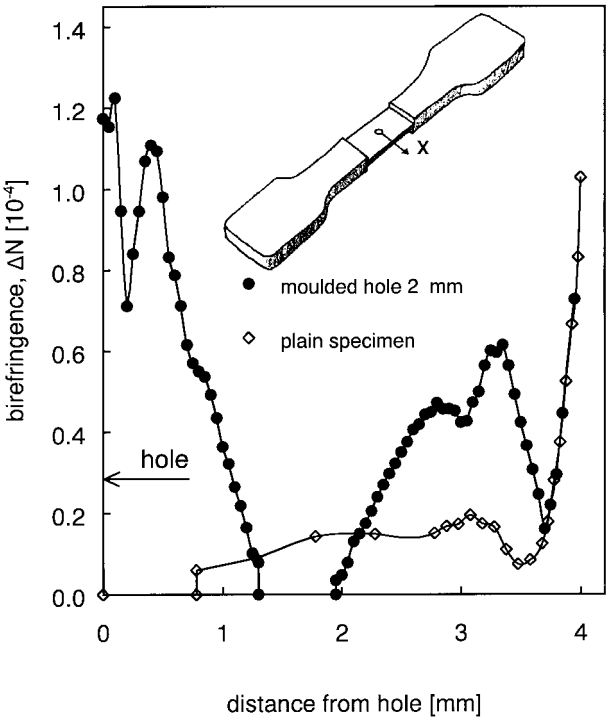

Figure 12 Birefringence distribution in the midplane of the specimen as indicated.

rates in three-point bending. There is no explanation for the fact that, unlike the tensile specimens with a fracture morphology of Figure 10(a), the fracture initiation point was not always at the edge of specimen side and hole surface.

Low Cycle Fatigue. The crack initiation point of the specimens tested in fatigue was always located at the hole surface. This is understandable, because in fatigue tests the load is lower than in tensile tests and the peak stress will be closer to the hole surface (Fig. 8). Therefore, specimens with a molded-in hole take most advantage of the molecular orientation.

At small amplitudes, the specimens with a drilled hole showed fracture initiation half-way along the hole and at higher amplitudes anywhere along the hole. Fracture surfaces of specimens with a molded-in hole showed resemblance to Figure 10(b). The crack initiation point was always located at the edge of the specimen side and hole surface.

CONCLUSIONS

Our results show that predictions of load-carrying ability at geometry transitions based on linear material behavior are safe, but conservative, even for a brittle material like PMMA. For high stress concentration factors, this approach is very conservative. This has been shown not only for short-term loads in tensile and three-point bending, but also for low cycle fatigue loading.

In particular, in the case of short-term loads, redistribution of stresses due to the nonlinear viscoelastic behavior must be taken into account. This result can explain the higher tensile strength of the grade H smooth specimens due to annealing below T_g, whereas the load-carrying ability of the specimens with a hole decreases by annealing. A notch factor or a notch sensitivity used by various authors[9,10] is a very inaccurate tool for modeling the load-carrying ability. However, an approach based on the actual stress field in combination with one or more critical material parameters is more promising.[22]

Furthermore, our results show that injection-molded products can amply profit from advantageous orientation due to the injection-molding process. This is shown by comparing specimens with drilled holes and molded-in holes in both short-term and fatigue loading. From the tensile tests, it is noted that molding-in a geometry transition yields more benefit for grade H specimens with higher molar mass than for grade L specimens. In the case of three-point bending specimens, the difference between drilled and molded-in holes seemed to increase for decreasing crosshead speeds. In the case of low cycle fatigue tests, at high amplitudes, the positive influence of the molded-in hole was partly reduced by the high coefficient of variation compared with the drilled specimens.

The specimens with a drilled hole and with a molded-in hole have different fracture surface morphologies. Particularly, the difference in location of fracture initiation is of importance, because it is an essential element of the fracture process. In the case of tensile specimens with a drilled hole, this location is determined by the highest stress and defects due to drilling. This is based on the observation of two different types of mirror zones. Presumably, the mirror zone of Figure 9(a) is typical for smooth geometry transitions in PMMA specimens. The crack initiation point of the latter was always half the wall thickness (i.e., in the area of minimum molecular orientation). In the case of specimens with a molded-in hole, the fracture initiation point may shift beyond the peak stress location, due to the molecular orientation around the hole. The extent of this shift depends on the sharpness of the stress distribution. The initiation point of the fracture surface in Figure 10(d) is located in the area of minimum molecular orientation as observed with the birefringence measurements in the midplane. In the case of tensile specimens with a molded-in hole, four different locations of fracture initiation were found. As the conditions lead toward more ductile behavior, the initiation point moves stepwise away from the hole surface, accompanied by lowering of the notch factor. This illustrates the complex relation between the injection molding process and the type of loading on the one hand and the load-carrying ability of plastic products on the other hand. However, to make a more accurate prediction of the load-carrying ability at geometry transitions, more knowledge of the deformation and fracture mechanism is necessary. Without such a model, the designer is forced to overdesign a product based on the safe linear elastic approach.

REFERENCES

1. S. Fellahi, A. Meddad, B. Fisa, and B. D. Favis, *Adv. Polym. Technol.,* **14,** 169 (1995).

2. R. J. Crawford, *Plastics and Rubber: Processing,* **June,** 61 (1980).
3. L. Schmidt, J. Opfermann, and G. Menges, *Polym. Eng. Rev.,* **1,** 1 (1981).
4. M. Demiray and A. I. Isayev, *SPE ANTEC,* **2,** 1576 (1996).
5. S. Y. Hobbs and C. F. Pratt, *J. Appl. Polym. Sci.,* **19,** 1701 (1975).
6. R. J. Crawford, V. Klewpatinond, and P. P. Benham, *Polymer,* **20,** 649 (1979).
7. Z. Bakerdjian and M. R. Kamal, *Polym. Eng. Sci.,* **17,** 96 (1977).
8. M. J. M. van der Zwet, *Deformation Yield and Fracture of Polymers,* P.R.I., London, 1994.
9. M. Takano and L. E. Nielsen, *J. Appl. Polym. Sci.,* **20,** 2193 (1976).
10. R. Prabhakaran, E. M. Somasekharan Nair, and P. Kumar Sinha, *J. Appl. Polym. Sci.,* **22,** 3011 (1978).
11. R. D. Goolsby and A. M. Chatterjee, *Polym. Eng. Sci.,* **23,** 117 (1983).
12. R. A. W. Fraser and I. M. Ward, *J. Mater. Sci.,* **9,** 1624 (1974).
13. G. Menges and H. Boden, in *Failure of Plastics,* W. Brostow and R. D. Corneliussen, Eds., Hanser Publishers, Munich, 1986, Chap. 9.
14. G. Nijman, Ph.D. thesis, University of Twente, The Netherlands, 1990.
15. L. Hoare and D. Hull, *Polym. Eng. Sci.,* **17,** 204 (1977).
16. P. Thienel, G. Wuebken, J. Opfermann, G. Ziegmann, K. de Zeeuw, K. Beyer, R. Krueger, N. Berndtsen, H. Berg, and G. Menges, *Kautschuk, Gummi, Kunststoffe,* **31,** 510 (1978).
17. A. J. Kinloch and R. J. Young, *Fracture Behaviour of Polymers,* Elsevier Applied Science, London, 1983, p. 252.
18. H. G. Moslé, O. S. Brüller, and H. Dick, *SPE ANTEC,* **38,** 290 (1980).
19. P. I. Vincent, *Polymer,* **1,** 425 (1960).
20. R. P. Kusy and D. T. Turner, *Polymer,* **17,** 161 (1976).
21. I. Narisawa, M. Ishikawa, and H. Ogawa, *J. Mater. Sci.,* **15,** 2059 (1980).
22. A. J. Heidweiller, *European Conference on Fracture 10,* K.-H. Schwalbe and C. Berger, Eds., EMAS, Warley, UK, 1994, p. 741.
23. R. P. Kambour, *J. Polym. Sci.: Macromol. Rev.,* **7,** 1 (1973).
24. M. J. M. van der Zwet, *European Conference on Fracture 9,* S. Sedmak, A. Sedmak, and D. Ružić, Eds., EMAS, Warley, UK, 1992, p. 196.
25. K. M. B. Jansen, Ph.D. thesis, Delft University of Technology, The Netherlands, 1993, p. 109.